

Laser Plasma Production of Metal–Corannulene Ion–Molecule Complexes

T. M. Ayers,[†] B. C. Westlake,[†] D. V. Preda,[‡] L. T. Scott,[‡] and M. A. Duncan^{*,†}

Department of Chemistry, University of Georgia, Athens, Georgia 30602-2556, and
Department of Chemistry, Merkert Chemistry Center, Boston College,
Chestnut Hill, Massachusetts 02467-3860

Received April 8, 2005

Gas-phase metal–corannulene ion–molecule complexes are produced by covaporization of materials in a laser plasma source and detected using a time-of-flight mass spectrometer. This is achieved by mixing metal, metal oxide, or organometallic powders with corannulene powder and covaporizing the mixture with 532 nm laser light. The mass spectra obtained reveal that transition metals and rare earths efficiently produce mono- and di-ligand complexes of the form $M^+(\text{cora})_n$, with $n = 1, 2$. Metal oxides are found to produce the mono-ligand complex with high efficiency. Covaporization of the organometallic π -complex iron cyclopentadienyl benzene with corannulene yielded both homoligand and heteroligand corannulene complexes. The binding energy of the iron cation to corannulene is suggested to be greater than its binding energy to benzene but less than its binding energy to cyclopentadiene.

Introduction

New techniques for metal vapor production and ligand aggregation schemes have made it possible to produce a fascinating variety of metal–aromatic complexes in the gas phase.¹ Clusters and complexes synthesized in these environments include metal–polycyclic aromatic hydrocarbon (PAH) complexes,^{2–8} metal–fullerene complexes,^{8–14} multimetal atom-coated fullerenes,^{15–19} and transition metal–aromatic multidecker sandwiches.^{20–28}

Although numerous examples of metal–aromatic complexes have been described, there is still much to learn about the structure and bonding of these systems. Recent work in our group has focused on new strategies for the production of metal–PAH complexes and the trends in complex growth and metal–aromatic bonding behavior.⁷ In this paper, we describe the production of a variety of metal complexes with the bowl-shaped corannulene molecule ($C_{20}H_{10}$).^{29–32}

PAHs occur naturally in environments wherever carbon is found. They are primarily formed in combustion processes including the burning of fossil fuels, forest fires, and cigarettes. Many PAHs are known carcinogens and have been linked to cancers of the respiratory and digestive systems.^{33,34} Due to their prevalence in nature,

- * Corresponding author. E-mail: maduncan@uga.edu.
[†] University of Georgia.
[‡] Boston College.
- (1) Martin, T. P. *Z. Phys. D Atom. Mol. Clusters* **1986**, *3*, 211.
 - (2) Buchanan, J. W.; Reddic, J. E.; Grieves, G. A.; Duncan, M. A. *J. Phys. Chem. A* **1998**, *102*, 6390.
 - (3) Buchanan, J. W.; Grieves, G. A.; Flynn, N. D.; Duncan, M. A. *Int. J. Mass Spectrom.* **1999**, *187*, 617.
 - (4) Foster, N. R.; Grieves, G. A.; Buchanan, J. W.; Flynn, N. D.; Duncan, M. A. *J. Phys. Chem. A* **2000**, *104*, 11055.
 - (5) Duncan, M. A.; Knight, A. M.; Negishi, Y.; Nagao, S.; Judai, K.; Nakajima, A.; Kaya, K. *J. Phys. Chem. A* **2001**, *105*, 10093.
 - (6) Foster, N. R.; Buchanan, J. W.; Flynn, N. D.; Duncan, M. A. *Chem. Phys. Lett.* **2001**, *341*, 476.
 - (7) Ayers, T. M.; Westlake, B. C.; Duncan, M. A. *J. Phys. Chem. A* **2004**, *108*, 9805.
 - (8) Buchanan, J. W.; Grieves, G. A.; Reddic, J. E.; Duncan, M. A. *Int. J. Mass Spectrom.* **1999**, *183*, 323.
 - (9) Wan, Z. M.; Christian, J. F.; Anderson, S. L. *Phys. Rev. Lett.* **1992**, *69*, 1352.
 - (10) Kan, S. Z.; Byun, Y. G.; Freiser, B. S. *J. Am. Chem. Soc.* **1994**, *116*, 8815.
 - (11) Kan, S. Z.; Byun, Y. G.; Freiser, B. S. *J. Am. Chem. Soc.* **1995**, *117*, 1177.
 - (12) Basir, Y.; Anderson, S. L. *Chem. Phys. Lett.* **1995**, *243*, 45.
 - (13) Reddic, J. E.; Robinson, J. C.; Duncan, M. A. *Chem. Phys. Lett.* **1997**, *279*, 203.
 - (14) Basir, Y. J.; Anderson, S. L. *Int. J. Mass Spectrom.* **1999**, *187*, 603.
 - (15) Martin, T. P.; Malinowski, N.; Zimmermann, U.; Naher, U.; Schaber, H. *J. Chem. Phys.* **1993**, *99*, 4210.
 - (16) Zimmermann, U.; Malinowski, N.; Naher, U.; Frank, S.; Martin, T. P. *Phys. Rev. Lett.* **1994**, *72*, 3542.
 - (17) Zimmermann, U.; Malinowski, N.; Burkhardt, A.; Martin, T. P. *Carbon* **1995**, *33*, 995.
 - (18) Martin, T. P.; Zimmermann, U.; Malinowski, N.; Heinebrodt, M.; Frank, S.; Tast, F. *Phys. Scr.* **1996**, *T66*, 38.

- (19) Tast, F.; Malinowski, N.; Frank, S.; Heinebrodt, M.; Billas, I. M. L.; Martin, T. P. *Z. Phys. D: At. Mol. Clusters* **1997**, *40*, 351.
- (20) Hoshino, K.; Kurikawa, T.; Takeda, H.; Nakajima, A.; Kaya, K. *Surf. Rev. Lett.* **1996**, *3*, 183.
- (21) Yasuike, T.; Nakajima, A.; Yabushita, S.; Kaya, K. *J. Phys. Chem. A* **1997**, *101*, 5360.
- (22) Kurikawa, T.; Takeda, H.; Hirano, M.; Judai, K.; Arita, T.; Nagao, S.; Nakajima, A.; Kaya, K. *Organometallics* **1999**, *18*, 1430.
- (23) Nakajima, A.; Nagao, S.; Takeda, H.; Kurikawa, T.; Kaya, K. *J. Chem. Phys.* **1997**, *107*, 6491.
- (24) Nagao, S.; Kurikawa, T.; Miyajima, K.; Nakajima, A.; Kaya, K. *J. Phys. Chem. A* **1998**, *102*, 4495.
- (25) Kurikawa, T.; Negishi, Y.; Hayakawa, F.; Nagao, S.; Miyajima, K.; Nakajima, A.; Kaya, K. *J. Am. Chem. Soc.* **1998**, *120*, 11766.
- (26) Miyajima, K.; Kurikawa, T.; Hashimoto, M.; Nakajima, A.; Kaya, K. *Chem. Phys. Lett.* **1999**, *306*, 256.
- (27) Nagao, S.; Kato, A.; Nakajima, A.; Kaya, K. *J. Am. Chem. Soc.* **2000**, *122*, 4221.
- (28) Nakajima, A.; Kaya, K. *J. Phys. Chem. A* **2000**, *104*, 176.
- (29) Barth, W. E.; Lawton, R. G. *J. Am. Chem. Soc.* **1966**, *88*, 380.
- (30) Lawton, R. G.; Barth, W. E. *J. Am. Chem. Soc.* **1971**, *93*, 1730.
- (31) Scott, L. T.; Hashemi, M. M.; Meyer, D. T.; Warren, H. B. *J. Am. Chem. Soc.* **1991**, *113*, 7082.
- (32) Scott, L. T.; Cheng, P. C.; Hashemi, M. M.; Bratcher, M. S.; Meyer, D. T.; Warren, H. B. *J. Am. Chem. Soc.* **1997**, *119*, 10963.
- (33) Guillen, M. D.; Sopelana, P.; Partearroyo, M. A. *Rev. Environ. Health* **1997**, *12*, 133.
- (34) Armstrong, B.; Hutchinson, E.; Unwin, J.; Fletcher, T. *Environ. Health Persp.* **2004**, *112*, 970.

the properties of PAH molecules have been explored extensively. The absorption, fluorescence, and phosphorescence of gas-phase PAH molecules and thin films are well documented.^{35–37} In astrophysics, PAHs have been implicated as components of dust grains in the interstellar medium (ISM). Ionized PAHs and metal–PAH complexes have also been suggested as possible carriers of the optical diffuse interstellar bands (DIBs)^{38–43} and the unidentified infrared bands (UIBs).^{43–46}

Metal–PAH complexes are important as models for surface science and catalysis; PAHs may be used to model finite sections of a carbon surface.^{47,48} There is also evidence that metal–PAH complexes may be constituents of interstellar gas clouds; they have been implicated in the depletion of atomic metal and silicon in the ISM⁴⁹ and as contributors to the DIBs and UIBs.⁵⁰ Increasing interest in metal–PAH systems has thus motivated many groups to produce these species in laboratory experiments. Dunbar and co-workers were the first to observe metal–PAH ion complexes in gas-phase experiments using FT-ICR mass spectrometry.⁵¹ From these experiments, they determined the binding kinetics of a variety of metal and nonmetal cations with PAHs. Our group has produced a variety of metal and multimetal–PAH sandwich complexes using laser vaporization of film-coated metal samples in a molecular beam cluster source.^{2–5} Competitive binding and photodissociation experiments were successful in determining structural information and relative bonding strengths of metals with benzene, C₆₀, and coronene.⁵ In other experiments, we used a laser desorption time-of-flight mass spectrometer to produce a variety of metal oxide and halide PAH complexes as well as mixed-ligand complexes.⁷ Experimental work has stimulated new theoretical studies investigating metal binding sites and bond energies on PAHs. Dunbar,⁵² Klippenstein and co-workers⁵³ and Jena and co-workers^{54,55} have been active in this area.

(35) Birks, J. B. *Photophysics of Aromatic Molecules*; John Wiley: London, 1970.

(36) Klessinger, M.; Michl, J. *Excited States and Photochemistry of Organic Molecules*; VCH Publishers: New York, 1995.

(37) Harvey, R. G. *Polyaromatic Hydrocarbons*; Wiley-VCH: New York, 1996.

(38) Bohme, D. K. *Chem. Rev.* **1992**, *92*, 1487.

(39) *The Diffuse Interstellar Bands*; Tielens, A. G. G. M., Snow, T. P., Eds.; Kluwer Academic Publishers: Dordrecht, 1995.

(40) Salama, F.; Bakes, E. L. O.; Allamandola, L. J.; Tielens, A. G. G. M. *Astrophys. J.* **1996**, *458*, 621.

(41) Henning, T.; Salama, F. *Science* **1998**, *282*, 2204.

(42) Salama, F. *Origins Life Evol. B* **1998**, *28*, 349.

(43) Ruiterkamp, R.; Halasinski, T.; Salama, F.; Foing, B. H.; Allamandola, L. J.; Schmidt, W.; Ehrenfreund, P. *Astron. Astrophys.* **2002**, *390*, 1153.

(44) Allamandola, L. J.; Tielens, A. G. G. M.; Barker, J. R. *Astrophys. J.* **1985**, *290*, L25.

(45) Allamandola, L. J.; Tielens, A. G. G. M.; Barker, J. R. *Astrophys. J. Suppl. Ser.* **1989**, *71*, 733.

(46) Leger, A.; Dhendecourt, L.; Defourneau, D. *Astron. Astrophys.* **1989**, *216*, 148.

(47) *Intercalation Chemistry*; Whittingham, M. S., Jacobson, A., Eds.; Academic Press: New York, 1982.

(48) *Graphite Intercalation Compounds and Applications*; Enoki, T., Suzuki, M., Endo, M., Eds.; Oxford University Press: New York, 2003.

(49) Klotz, A.; Marty, P.; Boissel, P.; Serra, G.; Chaudret, B.; Daudey, J. P. *Astron. Astrophys.* **1995**, *304*, 520.

(50) Klotz, A.; Marty, P.; Boissel, P.; deCaro, D.; Serra, G.; Mascetti, J.; deParseval, P.; Derouault, J.; Daudey, J. P.; Chaudret, B. *Planet. Space Sci.* **1996**, *44*, 957.

(51) Dunbar, R. C.; Uechi, G. T.; Asamoto, B. *J. Am. Chem. Soc.* **1994**, *116*, 2466.

(52) Dunbar, R. C. *J. Phys. Chem. A* **2002**, *106*, 9809.

(53) Klippenstein, S. J.; Yang, C. N. *Int. J. Mass Spectrom.* **2000**, *201*, 253.

Corannulene can be viewed as one-third of a C₆₀ molecule with the perimeter carbons terminated with hydrogens. Scott and co-workers discovered a simple and efficient synthetic route to corannulene,^{31,32} allowing for thorough exploration of its properties. Corannulene's unique bowl shape offers a variety of bonding possibilities for metal cations. Both η^5 and η^6 ring sites exist on the concave and convex sides of the molecule. Recent theoretical studies have shown that there is little preference for transition metal binding to the convex versus the concave sides of the molecule,^{52,55} in part because there is a low activation energy (0.43 eV) for bowl inversion.⁵⁶ However, cation binding to outside- η^6 sites is clearly preferred over binding to the central η^5 site. Several examples of synthetic inorganic complexes with corannulene derivatives illustrate this bonding preference.^{57–59} Bohme and co-workers have recently studied the reactivity of a variety of ligands with the iron–corannulene complex using a selected ion flowtube apparatus.⁶⁰ On the macroscale, Siegel and co-workers grew cocrystal polymeric arrays of silver perchlorate and other silver salts with corannulene.⁶¹ However, the bonds formed between silver and corannulene in the crystal are readily broken when this material is redissolved into solution. To our knowledge, the only other examples of metal–corannulene complexes that have been synthesized or reported in gas-phase experiments are those of Petrukhina, Scott, and co-workers.⁶²

The present work explores a general methodology for producing metal–corannulene ion–molecule complexes that may facilitate further studies of their properties. As shown below, laser ablation of samples combining corannulene with a variety of pure metal, metal oxide, or organometallic powders makes it possible to produce a variety of metal corannulene complexes.

Experimental Section

The laser desorption time-of-flight mass spectrometer used in these experiments has been described previously.⁶³ It has the capability for high acceleration fields (up to 30 kV) and delayed-pulsed ion extraction for improved resolution.⁶⁴ A 4.8 mm stainless steel flat-tipped probe is used for mounting the samples, which are mixed into a slurry with methanol (HPLC grade), applied with a pipet, and allowed to dry in air. Smooth sample surfaces are essential to obtain the best results in these laser desorption experiments. Once prepared, the samples are inserted into the mass spectrometer for analysis.

The metal powders studied in this experiment consist of the first-row transition metals titanium and chromium of varying

(54) Senapati, L.; Nayak, S. K.; Rao, B. K.; Jena, P. *J. Chem. Phys.* **2003**, *118*, 8671.

(55) Kandalam, A. K.; Rao, B. K.; Jena, P. Unpublished work, 2005.

(56) Scott, L. T.; Hashemi, M. M.; Bratcher, M. S. *J. Am. Chem. Soc.* **1992**, *114*, 1920.

(57) Seiders, T. J.; Baldrige, K. K.; O'Connor, J. M.; Siegel, J. S. *J. Am. Chem. Soc.* **1997**, *119*, 4781.

(58) Alvarez, C. M.; Angelici, R. J.; Sygula, A.; Sygula, R.; Rabideau, P. W. *Organometallics* **2003**, *22*, 624.

(59) Vecchi, P. A.; Alvarez, C. M.; Ellern, A.; Angelici, R. J.; Sygula, A.; Sygula, R.; Rabideau, P. W. *Angew. Chem., Int. Ed.* **2004**, *43*, 4497.

(60) Caraiman, D.; Koyanagi, G. K.; Scott, L. T.; Preda, D. V.; Bohme, D. K. *J. Am. Chem. Soc.* **2001**, *123*, 8573.

(61) Elliott, E. L.; Hernandez, G. A.; Linden, A.; Siegel, J. S. *Org. Biomol. Chem.* **2005**, *3*, 407.

(62) Petrukhina, M. A.; Andreini, K. W.; Mack, J.; Scott, L. T. *Angew. Chem., Int. Ed.* **2003**, *42*, 3375.

(63) Cornett, D. S.; Amster, I. J.; Duncan, M. A.; Rao, A. M.; Eklund, P. C. *J. Phys. Chem.* **1993**, *97*, 5036.

(64) Wiley, W. C.; McLaren, I. H. *Rev. Sci. Instrum.* **1955**, *26*, 1150.

grain sizes (Aldrich, Alfa Aesar). No care is taken to prevent these metals from oxidizing since it is also of interest to study metal oxide complexes with corannulene. Uranium is used as a representative of the actinide series; the source of uranium is the salt uranyl acetate, $\text{UO}_2(\text{CH}_3\text{CO}_2)_2 \cdot 2\text{H}_2\text{O}$. The organometallic tested is iron cyclopentadienyl benzene, $[\text{Fe}(\text{cp})(\text{bz})]\text{PF}_6$. Sodium and potassium cations are present as impurities in some experiments resulting from the handling of samples. Corannulene samples needed for this experiment were synthesized and purified by Scott and co-workers using previously described synthetic techniques.³² Pyrene, $\text{C}_{16}\text{H}_{10}$ (py), is also used in selected experiments. All other chemicals are used as received without further purification.

Desorption and ionization is accomplished by focusing (20 cm lens) the output of a Nd:YAG laser (Continuum MiniLite) operating at either 532 or 355 nm onto the sample on the probe tip inside the mass spectrometer. The fluence of the laser is adjusted with a variable attenuator prior to focusing to optimize production of the desired complexes. Consequently, energies less than 1 mJ/pulse are employed for most of these experiments. Once the material is vaporized, cations are accelerated down the flight tube at an energy of 10 keV and focused with an einzel lens before reaching the detector. Mass spectra are collected and averaged with a digital oscilloscope (LeCroy LT 341) and transferred to a PC via an IEEE-488 interface for processing.

Results and Discussion

Transition Metals + Corannulene. Covaporization of mixed powder samples has been demonstrated previously by our laboratory for the production of a variety of metal–PAH complexes of coronene, pyrene, etc.⁷ Here we employ the same methodology to produce metal–corannulene species. These experiments were carried out on selected first-row transition metals. Figure 1 shows a representative mass spectrum obtained from the vaporization (532 nm) of a mixed powder sample containing chromium and corannulene (upper trace) and chromium powder mixed with both corannulene and pyrene (lower trace). Only one atomic ion, chromium, is present in abundance in both spectra. Normally sodium and potassium atomic ions are present as a result of sample handling; however, no significant amounts are present in any of the spectra presented here. Also present in large abundance are chromium–PAH mono-ligand and di-ligand complexes. The di-ligand complexes here are presumed to be sandwiches because the PAH dimer intensities are always smaller in abundance than corresponding $\text{M}^+(\text{PAH})_2$ intensities. Results similar to the chromium data are obtained for other transition metals (e.g., vanadium and cobalt); the efficiency of complex formation varies with the metal used as we have described in previous work.⁷ We tried experiments using both the 532 and 355 nm outputs of the YAG laser for vaporization, but obtained useable signals only with the 532 nm wavelength. A wide variety of pulse energies were explored for both wavelengths, indicating that this was not an issue of power. Although 355 nm vaporization produced corannulene and corannulene dimer ions in large abundance, it was not successful in producing transition metal cations efficiently, which consequently prevents formation of metal–corannulene complexes. The 532 nm vaporization performed best at low pulse energies (0.5–1.0 mJ/pulse). At higher pulse energies, metal ions were detected, but complexes did not form efficiently, pre-

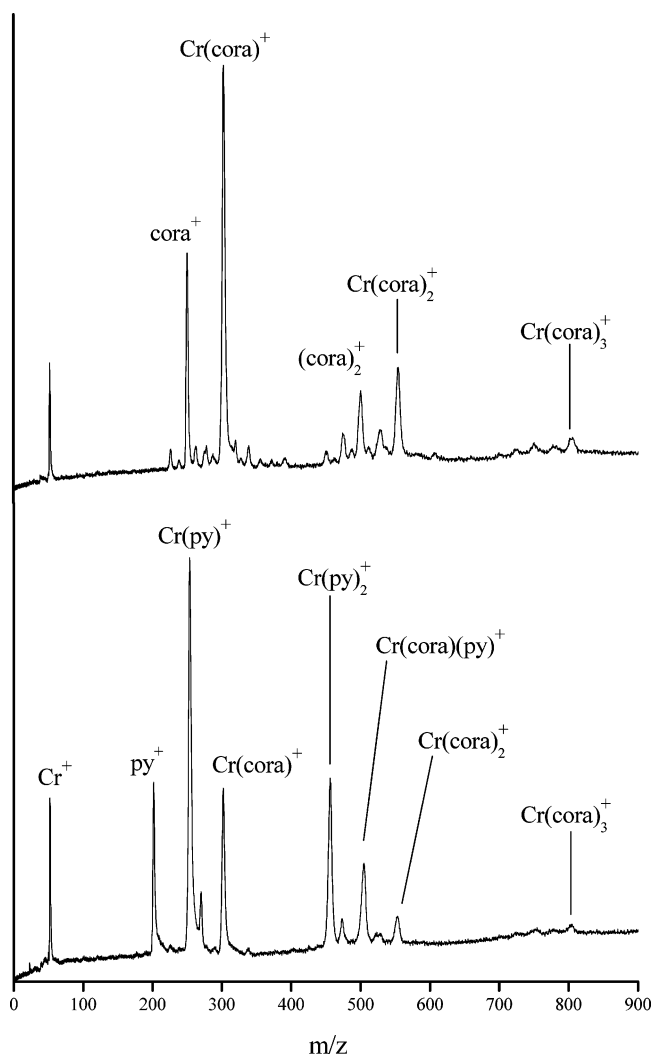


Figure 1. Mass spectrum resulting from covaporization of chromium powder and corannulene (top) and that resulting from covaporization of chromium powder and a mixture of corannulene and pyrene (bottom).

sumably because plasma conditions were too hot for efficient condensation reactions.

As shown in the lower trace, complexes are produced that contain either corannulene or pyrene as well as the mixed complexes containing both corannulene and pyrene, i.e., $\text{Cr}^+(\text{py})(\text{cora})$. Similar experiments produced mixed complexes with other PAH species such as coronene. Chromium shows no obvious preference for forming corannulene versus pyrene complexes, though the relative abundances in the spectrum presented are not equivalent for the $\text{Cr}^+(\text{py})_n$ and $\text{Cr}^+(\text{cora})_n$ ions. Experiments that varied the relative amounts of each PAH did seem to show larger abundances for corannulene complexes versus pyrene complexes (not shown), although it is difficult to be quantitative about this trend because the vaporization efficiency of the organics cannot be determined. In contrast to previous molecular beam experiments on transition metal–PAH complexes,^{2–6} we observe no multiple-metal complexes here with either corannulene or pyrene and the production of complexes with more than two PAH molecules is inefficient. In the molecular beam experiments, we employed a metal rod sample that was coated with a sublimed film of PAH. This film-coated sample was

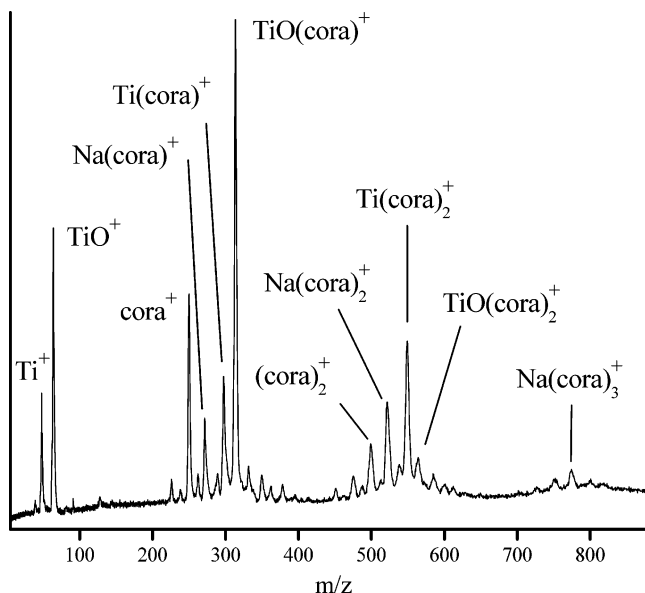


Figure 2. Mass spectrum resulting from covaporization of titanium powder and corannulene.

ablated in a laser vaporization source with a pulsed expansion gas, and complexes were allowed to grow in a channel extending beyond the vaporization position. The present experiment has neither an expansion gas nor a growth channel. The only opportunity for metal–PAH collisions occurs in the plume from the laser vaporization process, where conditions are substantially hotter than room temperature. It is therefore understandable that smaller complexes, on average, result from the present conditions. We also expect that complexes formed in the plasma must have substantial bond energies to survive these conditions.

Transition Metal Oxides + Corannulene. The early first-row transition metals titanium and vanadium produced metal oxide–corannulene complexes efficiently in these experiments. Figure 2 shows a mass spectrum obtained using titanium powder mixed with corannulene. Titanium and various titanium oxide ions are prevalent at low masses. Apparently, the oxygen arises from surface oxidation of the powder samples, which were handled in air. Both titanium mono-ligand and di-ligand complexes are observed, as are prominent adducts with Na^+ , even though the sodium is present only as an impurity. However, the most abundant complex produced is the titanium oxide mono-ligand complex, $\text{TiO}^+(\text{cora})$. The abundance of this ion can be rationalized to some degree because of the higher concentration of TiO^+ compared to Ti^+ . Additionally, it is likely that the metal oxide ion, which has partial ionic $\text{Ti}^{2+}, \text{O}^-$ character and a strong dipole moment, has a higher affinity for the organic π cloud than the bare metal ion. In contrast to these intensities observed for mono-ligand complexes, the spectrum shows a much larger abundance for the $\text{Ti}^+(\text{cora})_2$ di-ligand complex compared to that for the corresponding metal oxide ion. This behavior of oxide ion species with corannulene follows the same general pattern that we have observed previously in the clustering of transition metal chlorides and oxides with other PAH species.⁷ In several systems that we have studied, mono-ligand oxide or chloride complexes were formed in high abundance, but corresponding di-ligand species were formed either inef-

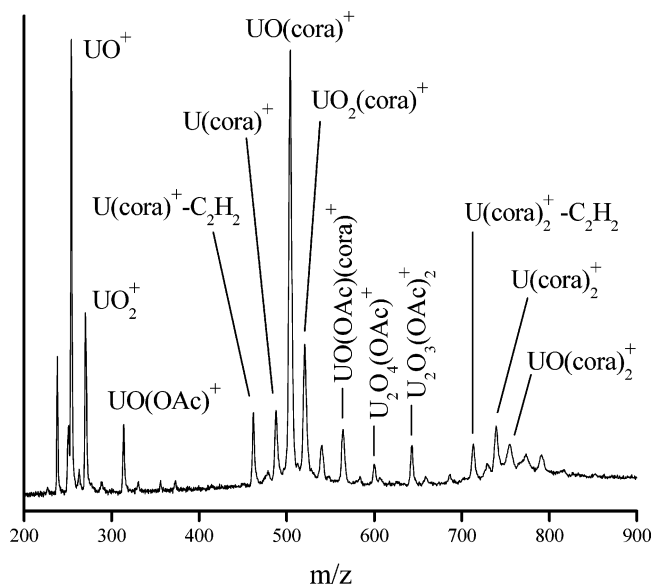


Figure 3. Mass spectrum resulting from covaporization of uranyl acetate and corannulene.

ficiently or not at all. This bonding pattern was explained by the different electrostatic interactions between the metal compound ions and the first and second PAH ligands. The first ligand interacts via strong attraction of the more positive end of the MO^+ or MX^+ ion for the negative π cloud of the PAH system. The more negative end of the oxide or halide ion is then left exposed, and this has an unfavorable interaction with the π cloud of a second potential PAH ligand. In fact, the second corannulene in the observed $\text{TiO}^+(\text{cora})_2$ species may even be associated with the exposed surface of the directly coordinated corannulene, rather than with the metal. This negative charge essentially screens the second PAH molecule from the metal and thus limits further complex formation. Apparently, a similar mechanism is at work here for corannulene complexes. This pattern of behavior is observed for both titanium and vanadium oxide complexes.

Uranium + Corannulene. To investigate other metals and their oxides, we examined uranium as a representative of the actinide series. Figure 3 shows the mass spectrum for covaporization experiments of uranyl acetate and corannulene. Large amounts of atomic uranium and uranium oxide ions are produced in the low mass range as well as the complex ion, uranium oxide acetate [$\text{UO}^+(\text{OAc})$]. Mono-corannulene complexes of these low mass range ions are also observed; the abundances of the smaller uranium ions correlate well with the abundances of mono-corannulene complexes produced. Uranium–corannulene di-ligand complexes are produced; however, the abundances observed do not match the abundances of the small mass range uranium ions as seen for the mono-corannulene complexes. In this series, pure metal di-corannulene, $\text{U}^+(\text{cora})_2$, is the most abundant ion, with uranium oxide corannulene di-ligand ions occurring in only low abundance. As in the case of the titanium oxide complexes, the exposed oxygen from the metal oxide–corannulene adduct apparently inhibits the binding of additional corannulene molecules.

Another interesting aspect of this spectrum is the observation of uranium–corannulene fragment ions.

Fragment ions corresponding to the loss of acetylene (C_2H_2) are observed for both the uranium mono- and di-ligand complexes. On the other hand, no significant amounts of fragment ions are detected from the uranium oxide complex ions. Similar behavior was also observed recently in molecular beam experiments in our lab for the photodissociation of uranium–benzene complex ions.⁶⁵ Benzene dissociation was found to occur when pure uranium–benzene complexes were photodissociated using 355 nm laser light, while photodissociation of uranium oxide–benzene complexes did not cause benzene fragmentation. Of the photofragments formed from uranium–benzene species, $U^+(C_4H_2)$ was the most abundant, presumably occurring by elimination of neutral C_2H_4 (ethylene), followed by $U^+(C_2H_2)$, corresponding to elimination of two acetylenes. However, in the case of corannulene, elimination of ethylene from the ring structure is less likely than elimination of acetylene, and only the latter channel is seen here. As seen in the benzene complexes, the oxide ions are apparently less reactive, because fragmentation in this way does not occur. It is also important to note that no corannulene fragments are observed for any of the other metals studied in these experiments. This suggests that uranium ion is more reactive with corannulene than the other metals used in this study.

Organometallics + Corannulene. We also investigated the covaporization of corannulene with other organometallics to attempt to produce mixed-ligand complexes. A limited number of mixed-ligand complexes of iron have been produced in conventional synthetic chemistry.^{66–68} However, these synthetic methods are problematic because of the poor solubility of many PAH systems. It is therefore interesting to see if covaporization methods would produce such mixed-ligand complexes. Here we focused on the iron cyclopentadienyl benzene cation, $Fe^+(cp)(bz)$, a species similar to ferrocene but with one of the cyclopentadiene ligands replaced by benzene. While ferrocene is an 18-electron species as a neutral complex, $Fe(cp)(bz)$ is an 18-electron species as a cation. The latter complex has a lower stability than ferrocene (it is highly photosensitive) and thus dissociates easily under our conditions. Figure 4 shows a mass spectrum of the covaporization of a mixed powder sample of $[Fe(cp)(bz)](PF_6)$ and corannulene. The primary fragments of the $Fe(cp)(bz)$ cation include Fe^+ and $Fe^+(cp)$ under all laser power conditions. The $Fe(cp)(bz)$ cation and ferrocene appear as the largest ions in abundance; decomposition of $Fe^+(cp)(bz)$ is the most likely source of ferrocene. The main complexes produced by the decomposition/reaction process in the plasma include $Fe^+(cora)$, $Fe^+(cp)(cora)$, and $Fe^+(cora)_2$. Thus, similar to the behavior we saw earlier for $Fe^+(cp)(coronene)$ complexes,⁷ mixed-ligand complexes with corannulene can indeed be produced with good yields.

The relative abundance of the different mixed-ligand and mono-ligand complexes can be rationalized simply on the basis of metal–ligand bond energies. The $Fe^+(cp)$ bond energy (91 kcal/mol)⁶⁹ is far greater than that

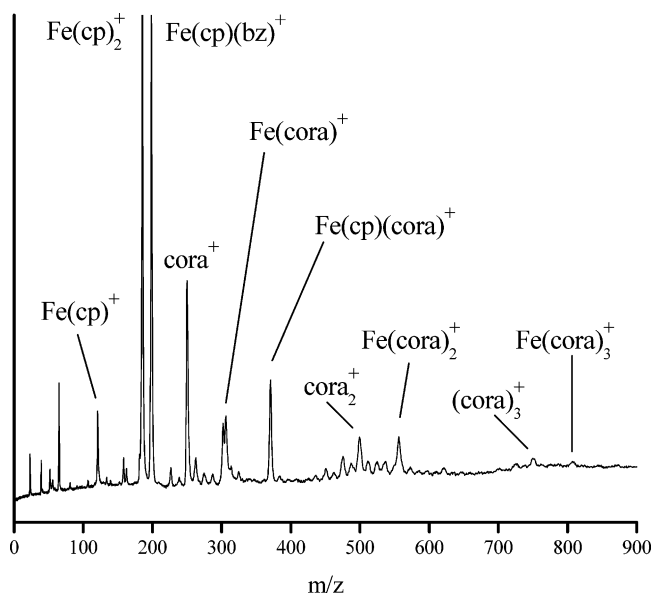


Figure 4. Mass spectrum resulting from covaporization of $Fe(cp)(bz)$ and corannulene.

of $Fe^+(bz)$ (37.8–44.7 kcal/mol),^{70,71} so therefore benzene is more likely to be eliminated first in the plasma dissociation of $Fe^+(cp)(bz)$. Consistent with this, the reaction product $Fe^+(cp)_2$ is produced in high abundance, but there is no $Fe^+(bz)_2$ observed. Likewise, $Fe^+(cp)(cora)$ is produced in a high abundance, but $Fe^+(bz)(cora)$ is not detected. This suggests that complex production involves the reaction of the fragments of $Fe^+(cp)(bz)$ with corannulene vapor created in the vaporization process. It is difficult to quantify the relative amount of corannulene vapor present compared to the amount of benzene and cyclopentadiene produced by the fragmentation of $Fe^+(cp)(bz)$. Because of this, the high abundance of ions such as $Fe^+(cp)_2$ could arise either because of their high stability or because of a bias in the concentration or reaction rate. However, the amount of Fe^+ , benzene, and cp must be comparable, since they arise from a common precursor. $Fe^+(cp)(cora)$ and $Fe^+(cora)_2$ are observed, while there are no benzene-containing ions detected at all except those from the precursor complex. Therefore, unless there is some unusual reaction rate effect that limits the complexation of Fe^+ with benzene (not likely based on our earlier work on this system⁷¹), these results indicate that corannulene binding to Fe^+ must be considerably stronger than the binding of benzene. Consistent with this, Jena and co-workers have recently calculated the $Fe^+(cora)$ bond energy to be approximately 84 kcal/mol,⁵⁵ which is indeed greater than the $Fe^+(bz)$ bond energy.

Complex Growth and Structures. As we have shown above, a variety of mono-ligand and sandwich complexes of corannulene can be produced by these laser plasma methods and detected by mass spectrometry. It is only natural to speculate about the structures of these complexes, although mass spectrometry does not provide any specific structural insight. If we accept the predic-

(65) Pillai, E. D.; Molek, K. S.; Duncan, M. A. *Chem. Phys. Lett.* **2005**, *405*, 247.

(66) Morrison, W. H.; Ho, E. Y.; Hendrickson, D. N. *Inorg. Chem.* **1975**, *14*, 500.

(67) Schmitt, G.; Keim, W.; Fleischhauer, J.; Walbergs, U. *J. Organomet. Chem.* **1978**, *152*, 315.

(68) Astruc, D. *Tetrahedron* **1983**, *39*, 4027.

(69) Lewis, K. E.; Smith, G. P. *J. Am. Chem. Soc.* **1984**, *106*, 4650.

(70) Meyer, F.; Khan, F. A.; Armentrout, P. B. *J. Am. Chem. Soc.* **1995**, *117*, 9740.

(71) Jaeger, T. D.; van Heijnsbergen, D.; Klippenstein, S. J.; von Helden, G.; Meijer, G.; Duncan, M. A. *J. Am. Chem. Soc.* **2004**, *126*, 10981.

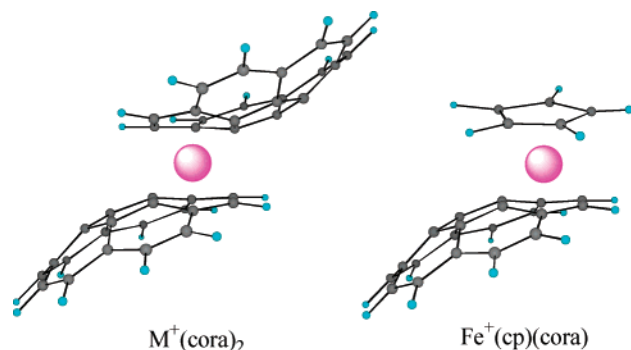


Figure 5. Schematic structures expected for various complexes studied here. (a) Di-ligand complex $M^+(\text{cora})_2$. The binding to outer rings (convex η^6 sites) on both corannulene molecules leads to an expected staggered sandwich structure. (b) $Fe^+(\text{cp})(\text{cora})$ mixed sandwich, also with outer ring η^6 binding on corannulene.

tions of theory and existing experimental results, then metal ion binding to corannulene should take place on the convex side in one of the outer η^6 ring sites rather than on the η^5 interior site.^{52,55,57–59} If this is true, then $M^+(\text{cora})_2$ sandwich complexes are unlikely to be symmetrical. Because the metal ion will likely induce significant polarization in the organic π system, the ends of the corannulene molecule opposite the metal sites should become more electron deficient, and then these like-charged objects would tend to avoid each other in space. Figure 5 shows the sandwich structure that would most likely result from this, which has a staggered conformation for the two corannulene rings as opposed to an eclipsed conformation that could be reached by rotation around the ligand–metal bond. We have previously proposed such staggered sandwich structures for metal–coronene sandwich complexes.⁴ The second structure in the figure shows a similar arrangement that would result for $M^+(\text{cp})(\text{cora})$ mixed sandwiches. This kind of structure has in fact been determined for $M(\text{cp})(\text{coronene})$ complexes.^{66–68} It will be interesting to see if future spectroscopic studies can confirm these predicted structures.

Another interesting aspect of these studies is that no significant amounts of multiple metal–corannulene complexes were observed. This is in contrast to molec-

ular beam experiments performed by our group, where many multimetal complexes are seen.^{2–5,8} The simplest reason for this difference is the low metal concentration and the absence of a collision gas in the present experiments. In these experiments, temperatures generated in the cluster source are much higher than in pulsed nozzle experiments, and the vaporized species also experience fewer collisions. Thus, only small clusters with relatively high bond energies survive. It may be possible in the future to explore other cluster production methods that include higher metal concentrations and collisional stabilization to explore templating effects, if any, that may occur for the binding of multiple metals on the corannulene surface.

Conclusions

We describe the production of a variety of ion–molecule complexes between metal cations and corannulene. These complexes are produced using laser vaporization of mixed powder samples of corannulene combined with pure metal, metal oxides, or organometallic complexes. We do not observe efficient production of multiple metal atom corannulene complexes. Likewise, we do not see efficient production of systems with more than two corannulene molecules. These more highly aggregated systems can be formed in molecular beam experiments, where expansion gases are present and provide a means for collision stabilization. However, we do form a wide variety of metal and metal compound complexes as well as mixed-ligand species with two corannulene species or with one corannulene and cyclopentadiene. Similar behavior was also observed with other PAH molecules using the same laser vaporization techniques.⁷ This method of complex formation is therefore versatile and can be implemented in many different mass spectrometers to enable studies of reaction kinetics and ligand displacement processes in these systems.

Acknowledgment. This work is supported by the Air Force Office of Scientific Research (grant F49620-00-1-0118 to M.A.D.) and the Department of Energy (grant DE-FG02-93ER14359 to L.T.S.). We also appreciate preliminary communication of theoretical results provided by Jena and co-workers.

OM050267C